ELSEVIER

Journal of Electroanalytical Chemistry 394 (1995) 253–262

JOURNAL OF ELECTROANALYTICAL CHEMISTRY

Reactions involving H, OH and O species on rhodium in $H_2SO_4 \cdot 12H_2O$ and $HClO_4 \cdot 5.5H_2O$ in the range 198–298 K

M.I. Florit, A.E. Bolzán, A.J. Arvia *

Instituto de Investigaciones Fisicoquímicas Teóricas y Aplicadas (INIFTA), Facultad de Ciencias Exactas, Universidad Nacional de La Plata, Sucursal 4, Casilla de Correo 16, (1900) La Plata, Argentina

Received 4 October 1994; in revised form 14 February 1995

Abstract

The voltammetric behaviour of polycrystalline rhodium in $H_2SO_4 \cdot 12H_2O$ and $HClO_4 \cdot 5.5H_2O$ was investigated by conventional and triangularly modulated voltammetry in the range 198–298 K. H and OH electrosorption reactions and a fast electrochemical process in the potential range preceding the oxygen evolution reaction (OER) were studied. For both electrolytes, as the temperature diminished, the H atom reactions and those reactions related to the O-containing surface species became increasingly irreversible, whereas the fast electrochemical process preceding the OER was nearly the same, irrespective of the temperature. Explanations recently advanced for the behaviour of Rh in more diluted solutions of the same acids at 298 K and the electrochemical behaviour of the different processes are discussed, considering mainly the effects of sulphate anion adsorption and perchlorate anion decomposition on Rh.

Keywords: Hydrogen; Hydroxide; Oxygen; Rhodium; Voltammetry; Electrosorption; Sulplate; Perchlorate

1. Introduction

The effect of temperature on the kinetics of electrochemical reactions has been studied during the last decades, particularly to evaluate the temperature dependence of Tafel slopes and its relation to electron transfer theory [1]. More recently, the hydrogen electrode reaction (HER) on Pt in $HClO_4 \cdot 5.5H_2O$ in the range 189–292 K [2,3] and the voltammetric behaviour of H and O adatoms on Pt in $H_2SO_4 \cdot 12H_2O$ and $HClO_4 \cdot 5.5H_2O$ in the range 189–292 K [4,5] have received special consideration. Although restricted to Pt, these results are highly interesting when exploring new aspects related to the structure of the metal|solution interface in relation to the kinetics of electrocatalytic processes.

The voltammetric response of H and O atom electrosorption reactions on Rh in both acid and alkaline solutions in the range 273–373 K [6–11] indicates a marked effect on the kinetics of those reactions by the composition of the electrolyte solution—particularly on the anion adsorption [12–16], electrode potential and temperature (T). The effect of these variables follows the change in the adsorption characteristics of anions in the solution [10], although data on the effect of T on these reactions are very scarce. Previous results reported for Rh in 2.3 M H_2SO_4 indicated that an increase in temperature from 263 to 363 K resulted in a decrease in the electroformation threshold potential of the O-containing layer [6]. The reaction itself was confined to a narrower and lower potential range. The problem posed then is to understand how the effect of T on these reactions manifests in the low temperature range.

This paper describes a voltammetric study of reactions which, on platinum metals such as Rh, usually proceed in the potential range of the H and O electrosorption reactions, and fast redox processes preceding the oxygen evolution reaction (OER). These reactions are studied on polycrystalline Rh in $H_2SO_4 \cdot 12H_2O$ and $HClO_4 \cdot 5.5H_2O$ covering the ranges 198–298 K and 210–298 K, respectively, in which the electrolyte composition of both systems remains constant.

2. Experimental

A three-electrode glass electrochemical cell (as described elsewhere [4]) was used. The working electrode consisted of a polycrystalline Rh wire (Johnson Matthey,

* Corresponding author.

SSDI 0022-0728(95)03983-X

99.998% purity, either 0.63 or 0.53 cm^2 in geometric area). The working electrode was surrounded by a Pt foil which served as the counter-electrode. The reference electrode was a Pd–H_2 electrode that ended in a Luggin–Haber capillary tip, which was placed axially to the working electrode at a distance of about 1 mm. Potentials (E) in the text are referred to the reversible hydrogen electrode scale at T.

The $H_2SO_4 \cdot 12H_2O$ and $HClO_4 \cdot 5.5H_2O$ were prepared from H_2SO_4 (97%) and $HClO_4$ (70%) acids (Merck, p.a.) and Milli-Q* water. The composition of these electrolytes was constant on changing from the liquid to solid. The Cl^- ion content in the $HClO_4 \cdot 5.5H_2O$ was less than 5×10^{-5} M. The cell temperature was monitored by means of a precision thermistor (YSI 44001) and kept constant at ± 0.5 K using a Lauda model WK120 Ultra-Kryomat. A slow cooling rate ensured that a completely frozen electrolyte layer remained attached to the electrode surface when T was below the electrolyte freezing temperature ($T_f(H_2SO_4 \cdot 12H_2O) = 199.5$ K; $T_f(HClO_4 \cdot 5.5H_2O) = 228$ K). Conventional voltammetry was performed at 0.1 V s^{-1}, covering different potential regions within the threshold potentials of the HER and OER.

To detect the presence of reversible electrochemical processes, the triangularly modulated linear sweep voltammetry (TMV) technique was applied. The background of this technique has been extensively described in the literature [17,18] and it has been used successfully to detect fast conjugated surface electrochemical reactions, such as those involved in the electrosorption of H and O atoms at both the monolayer and multilayer level [17,19,20]. In this case, the TMV modulation frequency f was varied in the range $20 \leq f \leq 1000$ Hz, whereas the modulation amplitude A was fixed at 0.040 V. For the triangularly modulated voltammograms, either a single linear or a triangular scan was recorded on a Kenwood model CS-5130 oscilloscope and photographed with a Micro Nikkor 55 mm f 2.8 lens mounted on a Nikon FE2 camera using Ilford FP4 film.

All the experiments were performed under purified N_2, covering the range 298–198 K for $H_2SO_4 \cdot 12H_2O$ and the range 298–210 K for $HClO_4 \cdot 5.5H_2O$.

3. Results

3.1. Voltammetry in $H_2SO_4 \cdot 12H_2O$ at different temperatures

At 298 K, the stabilized voltammogram of Rh in $H_2SO_4 \cdot 12H_2O$, obtained at 0.1 V s^{-1} between 0.07 and 1.40 V, exhibits two well-defined potential regions (I and II) (Fig. 1). At potentials below 0.40 V (region I), a pair of reversible conjugated current peaks can be observed at about 0.135 V, which are related to H atom electrosorption on Rh. Both current peaks show a shoulder at about 0.2 V. Furthermore, the HER starts at potentials below 0.1 V.

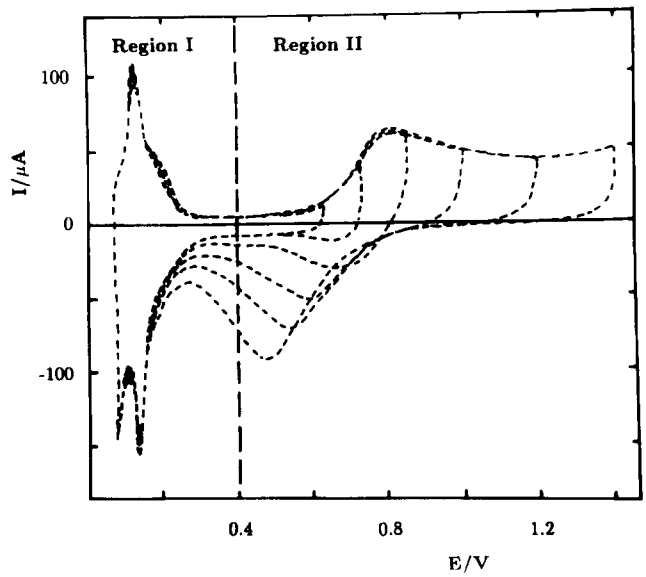

Fig. 1. Potentiodynamic $E-I$ profiles of polycrystalline Rh in $H_2SO_4 \cdot 12H_2O$ at $v = 0.1$ V s^{-1} and $T = 298$ K between $E_c = 0.07$ V and E_a changed stepwise from 1.40 to 0.65 V. Apparent electrode area, 0.63 cm^2.

Region II comprises the electroformation of the O-containing layer on Rh, which commences at about 0.58 V. This complex reaction is characterized by a broad positive current peak at about 0.8 V, followed by a very smooth current decay for $E \approx 1.2$ V, and a slight current increase for $E > 1.2$ V. A broad negative current peak located at about 0.47 V, related to the electroreduction of the O-containing layer, is recorded during the reverse potential scan. The corresponding peak potential shifts negatively as the upper switching potential (E_a) is positively increased, as a result of the increasing irreversibility of the electrochemical reaction itself. This electroreduction process overlaps considerably the initial stages of the H electroadsorption reaction.

Fast redox processes related to oxide film formation on Rh can also be followed by TMV. Thus, TMV carried out from 0.05 to 1.4 V at $f = 100$ Hz and $A = 0.040$ V shows two fast conjugated current envelopes (Fig. 2(a)). The first reversible envelope which appears in the range $0.08 \leq E \leq 0.28$ V (region I) can be assigned to fast H atom electrosorption reactions; the corresponding anodic (positive) to cathodic (negative) apparent charge ratio is $q_a/q_c \approx 1$. The symmetric second reversible envelope observed in the range $0.5 \leq E \leq 1.0$ V (region II) can be associated with the beginning of the formation of the O-containing layer on the Rh [8]. In this case, $q_a/q_c \approx 1.1$ for $f = 100$ Hz. The value of q_a is smaller than that involved in the H electrosorption process, probably because of the relatively high surface coverage by adsorbed HSO_4^- and SO_4^{2-} ions (hereafter denoted as sulphate anions); this adsorption takes place in this potential range, as has been recently concluded by other authors [13–16]. This fact can explain

why the reverse TMV scan (Fig. 2(b)) is more poorly defined, because it exhibits a smooth positive peak at about 0.68 V and an asymmetric negative peak at about 0.54 V. In this case, $q_a/q_c \approx 0.5$, and the peak potential difference is $\Delta E \approx 0.2$ V. These results suggest that the electroreduction process behaves irreversibly. Conversely, the first reversible system in region I is nearly the same as that in Fig. 2(a), because the effect of the reversible adsorption of sulphate anions on the H atom electrosorption rapidly decreases from 0.25 to 0 V [13].

In contrast, when the potential scan reaches a value close to 2 V (Fig. 3) an ill-defined positive current contribution appears at about 1.6 V, i.e. prior to the OER threshold potential. The Rh oxide film which is produced at high positive potentials is electroreduced below the potentials required for those oxide layers formed at lower potentials. Furthermore, the current peak of the oxide film electroreduction is preceded by a negative limiting current which extends from 1.5 to 0.8 V.

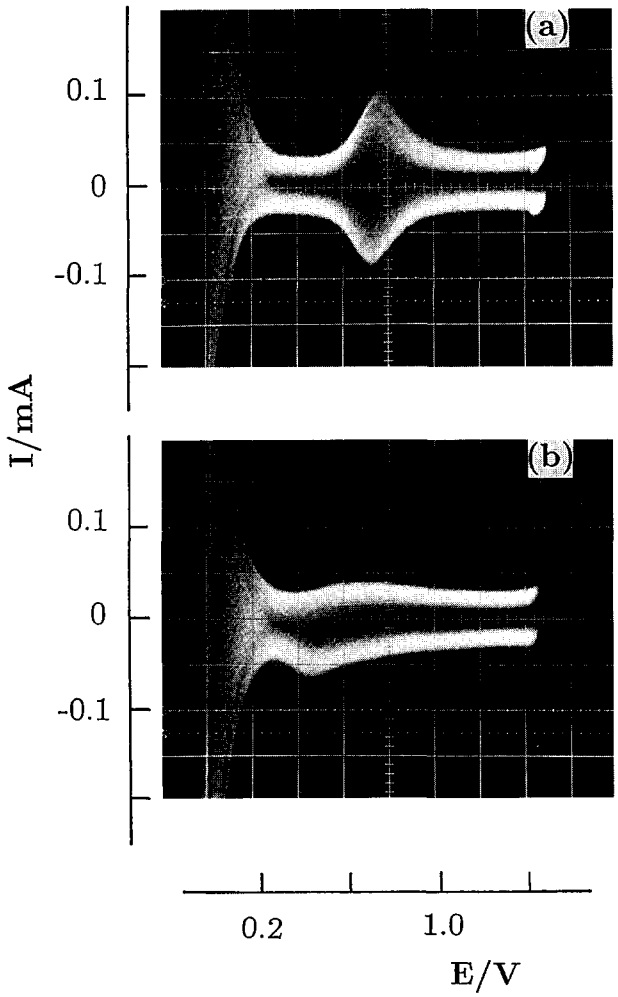

Fig. 2. Triangularly modulated voltammogram recorded between 0.06 and 1.42 V at 0.1 V s^{-1} and $T = 298$ K in $H_2SO_4 \cdot 12H_2O$ with $A = 0.040$ V and $f = 1$ kHz: (a) positive-going potential scan; (b) negative-going potential scan. Apparent electrode area, 0.63 cm^2.

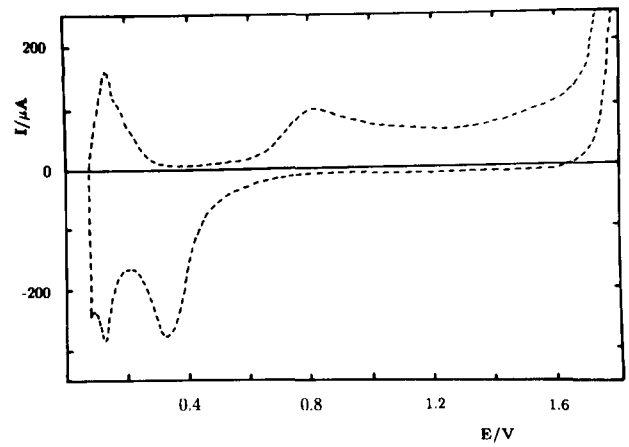

Fig. 3. Potentiodynamic $E-I$ profiles of polycrystalline Rh in $H_2SO_4 \cdot 12H_2O$ at $v = 0.1$ V s^{-1} and $T = 298$ K between $E_c = 0.07$ V and $E_a = 1.80$ V. Apparent electrode area, 0.63 cm^2.

The TMV carried out from 0 to 2 V shows a new fast conjugated system at about 1.7 V, i.e. in the potential range just preceding the commencement of the OER (Fig. 4). This new system appears during both the positive- and the negative-going potential scans. Furthermore, it is found that $q_a/q_c \approx 1$, but the anodic charge is only a fraction (0.6) of the charge involved in the positive current peak observed at 0.75 V. In addition, the complex contour of the H adatom electrosorption involves reversible conjugated current peaks at about 0.38 and 0.1 V.

As T is decreased from 278 to 210 K, the entire voltammogram obtained at 0.1 V s^{-1} changes, particularly in the H atom electrosorption potential range. Thus, on decreasing T from 253 to 210 K (Fig. 5), both the positive and negative charges related to the H atom electrosorption diminish and a new current contribution is enhanced at more positive potentials. The electrochemical reactions are less reversible, covering a wider potential range. According to the behaviour of Rh in more dilute aqueous H_2SO_4 at 298 K [13–16], the hysteresis shown in Fig. 5 indicates a predominant effect of sulphate anion adsorption as the temperature is decreased. The broadening of the H atom region on the positive-going scan compared with the narrow peak on the reverse scan has been shown to result from the fact that an anion is more difficult to desorb from a positively charged surface (negative-going potential scan) compared with the adsorption of an anion on an already negatively charged surface (positive-going potential scan) [15,16].

The stabilized cyclic voltammogram of Rh in frozen $H_2SO_4 \cdot 12H_2O$ ($T = 198$ K) obtained between 0.06 and 1.45 V at 0.1 V s^{-1} exhibits two broad peaks in the H adatom potential region, followed by a very broad current peak in region II (Fig. 6(a)). The reverse scan shows a broad negative peak, resulting from the electroreduction of the O-atom-containing layer, as well as another large negative contribution in region I (Fig. 6(b)). As E_a is

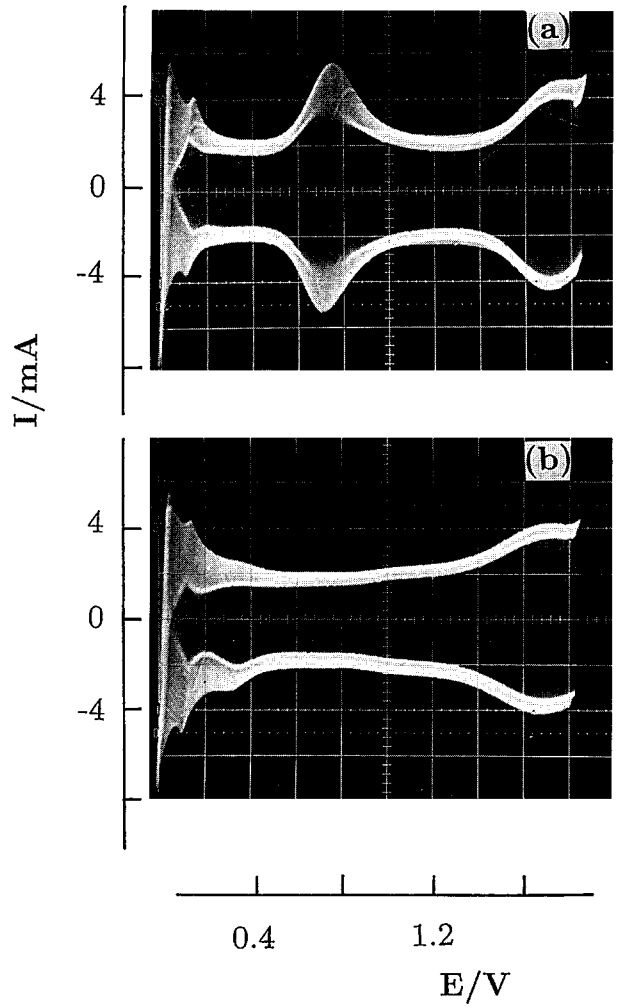

Fig. 4. Triangularly modulated voltammogram recorded between 0.06 and 1.80 V at 0.1 V s^{-1} and $T = 278$ K in $H_2SO_4 \cdot 12H_2O$ with $A = 0.040$ V and $f = 1$ kHz: (a) positive-going potential scan; (b) negative-going potential scan. Apparent electrode area, 0.63 cm^2.

decreased stepwise from 1.45 to 0.55 V, the electroreduction current peak of the O-containing layer shifts positively and the negative charge in region I related to H atom electroadsorption is reduced appreciably (Fig. 6(b)). In fact, no negative current peak can be observed when $E_a < 0.6$ V, i.e. when E_a lies in the potential range of maximum adsorption for sulphate anions on Rh [13] and the O atom layer electroformation is avoided (Fig. 6(b)). Furthermore, as $E_c \rightarrow 0$ V, where E_c is the lower switching potential, the positive peak located at about 0.125 V—which corresponds to the electro-oxidation of molecular H_2 formed in the preceding negative-going potential scan—is clearly observed.

The TMV response of Rh in frozen $H_2SO_4 \cdot 12H_2O$ provides additional information only when $f \leq 100$ Hz. Otherwise, for $f > 100$ Hz, a trend towards featureless voltammograms is observed, consisting mainly of a capacitive response. Thus, TMV carried out from 0 up to 2 V at $f = 20$ Hz and $A = 0.040$ V shows three main current

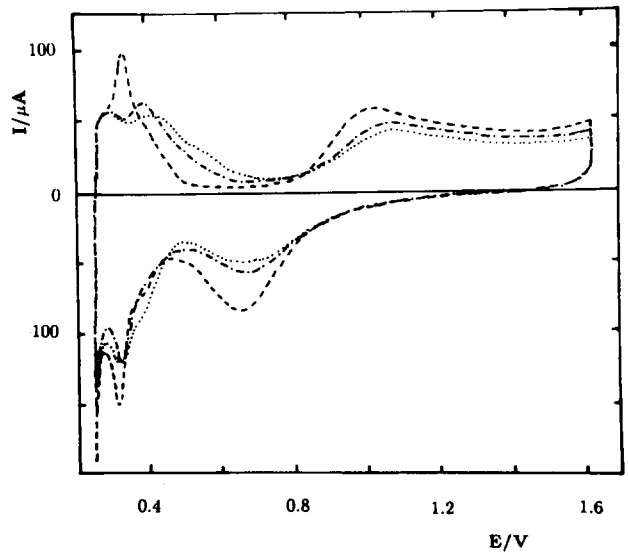

Fig. 5. Potentiodynamic $E-I$ profiles of polycrystalline Rh in $H_2SO_4 \cdot 12H_2O$ at $v = 0.1$ V s^{-1} between $E_c = 0.05$ V and $E_a = 1.45$ V: – – –, $T = 253$ K; –·– $T = 233$ K; · · · $T = 210$ K. Apparent electrode area, 0.63 cm^2.

contributions (Fig. 7). The first contribution at about 0.1 V is presumably related to the electro-oxidation of traces of H_2 formed during the preceding negative-going potential

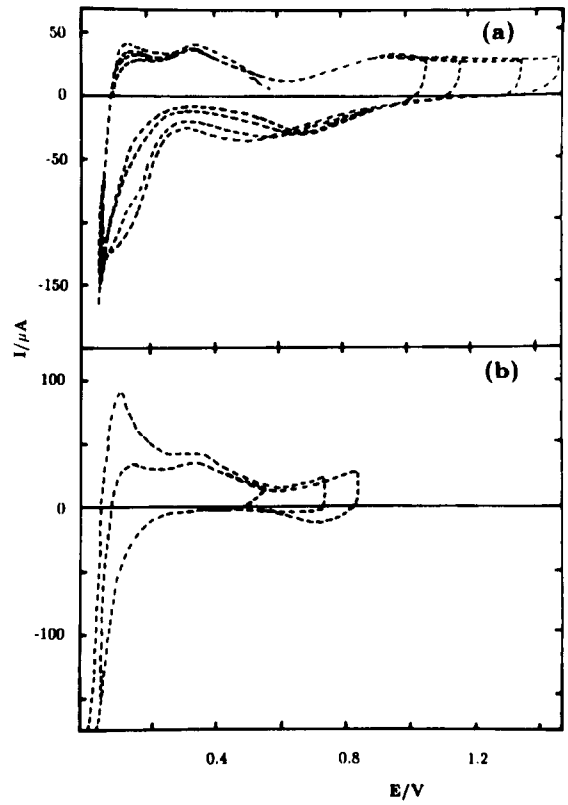

Fig. 6. Potentiodynamic $E-I$ profiles of polycrystalline Rh in $H_2SO_4 \cdot 12H_2O$ at $v = 0.1$ V s^{-1} and $T = 198$ K between $E_c = 0.05$ V and E_a changed stepwise from 1.45 to 0.55 V. Apparent electrode area, 0.63 cm^2.

scan; the second contribution at about 0.3 V (region I) involves a conjugated pair of current envelopes related to the H atom electrosorption affected by the adsorption of sulphate anions; the third contribution also involves a pair of conjugated current envelopes (region II) which correspond to the initial stages of the O-containing layer electroformation and/or electroreduction. Subsequently, the reverse scan (Fig. 7(b)) presents several ill-defined negative and positive current contributions. The first pair of envelopes located at about 0.8 V comprises a charge smaller than that resulting in Fig. 7(a). Subsequently, electrosorption processes take place in the potential range where strong sulphate anion adsorption occurs [13]. Further details of these reactions result from TMV carried out for $E_c = 0$ V and $E_a = 0.58$ V at $f = 50$ Hz (Figs. 7(c) and 7(d)). Therefore, TMV carried out from 0.58 to 0 V (Fig. 7(d)) shows the absence of reversible conjugated current peaks attributable to H adatom reactions, whereas TMV from 0 to 0.58 V (Fig. 7(c)) shows a single pair of conjugated current peaks at about 0.2 V. Finally, when the potential scan exceeds the OER threshold potential (Fig. 8), TMV shows that the second redox system becomes a fast process similar to that found at 298 K.

Therefore, the voltammetric features of Rh in $H_2SO_4 \cdot 12H_2O$ confirm that sulphate anion adsorption has a remarkable effect on the voltammetric response of the H atom and O-containing layer formation. These reactions show an increasing irreversibility as T is reduced, whereas there is only a minor effect of T on the redox system observed at about 1.8 V.

3.2. Voltammetry in $HClO_4 \cdot 5.5H_2O$ at different temperatures

A voltammogram of Rh in $HClO_4 \cdot 5.5H_2O$ at 298 K (Fig. 9) obtained at 0.1 V s^{-1} between 0.1 and 1.55 V, shows electrochemical reactions taking place in two main potential regions (I′ and II′), as previously described for $H_2SO_4 \cdot 12H_2O$, although the current contribution in region I′ for $HClO_4 \cdot 5.5H_2O$ is narrower than that in region

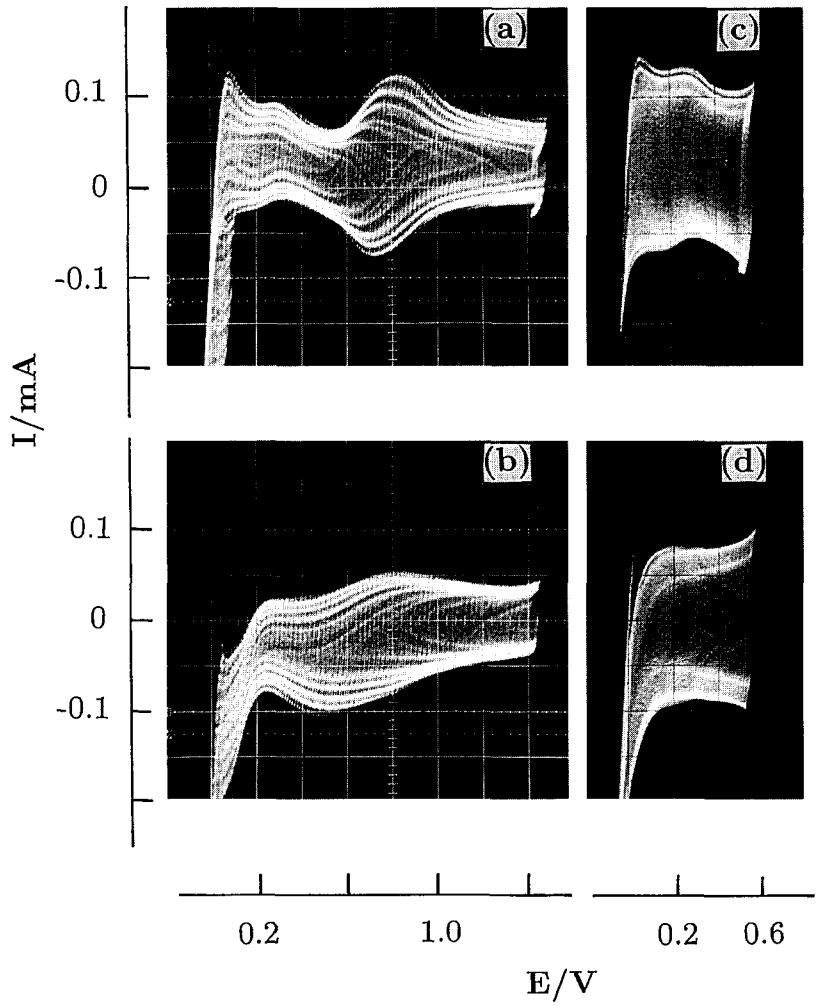

Fig. 7. Triangularly modulated voltammogram recorded (a), (b) between 0.05 and 1.45 V and (c), (d) between 0.0 and 0.55 V at 0.1 V s^{-1} and $T = 198$ K in $H_2SO_4 \cdot 12H_2O$ with $A = 0.040$ V, (a), (b) $f = 20$ Hz and (c), (d) $f = 50$ Hz: (a), (c) positive-going potential scan; (b), (d) negative-going potential scan. Apparent electrode area, 0.63 cm^2.

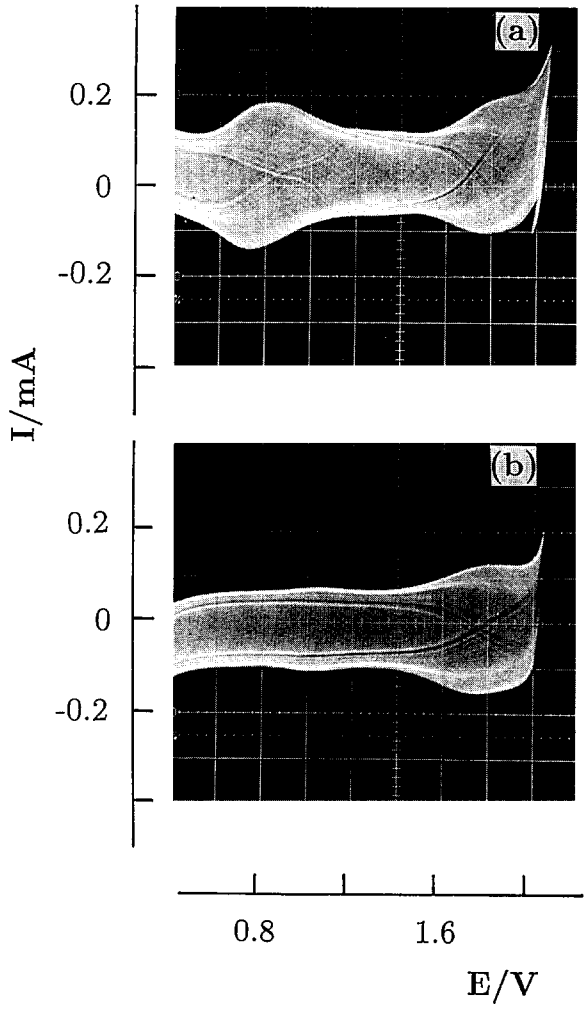

Fig. 8. Triangularly modulated voltammogram recorded between 0.40 and 2.0 V at 0.1 V s^{-1} and $T = 198$ K in $H_2SO_4 \cdot 12H_2O$ with $A = 0.040$ V and $f = 50$ Hz: (a) positive-going potential scan; (b) negative-going potential scan. Apparent electrode area, 0.63 cm^2.

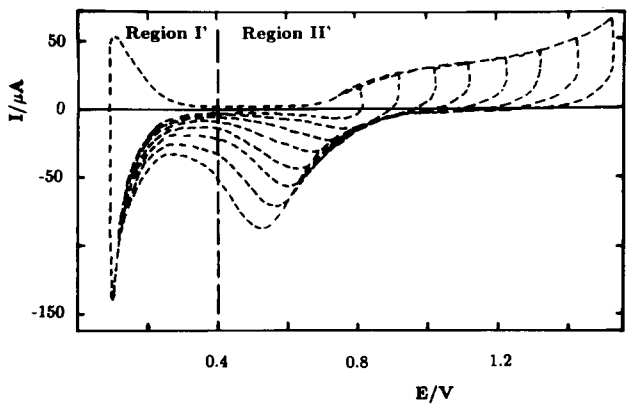

Fig. 9. Potentiodynamic $E-I$ profiles of polycrystalline Rh in $HClO_4 \cdot 5.5H_2O$ at $v = 0.1$ V s^{-1} and $T = 298$ K between $E_c = 0.07$ V and E_a changed stepwise from 1.40 to 0.65 V. Apparent electrode area, 0.53 cm^2.

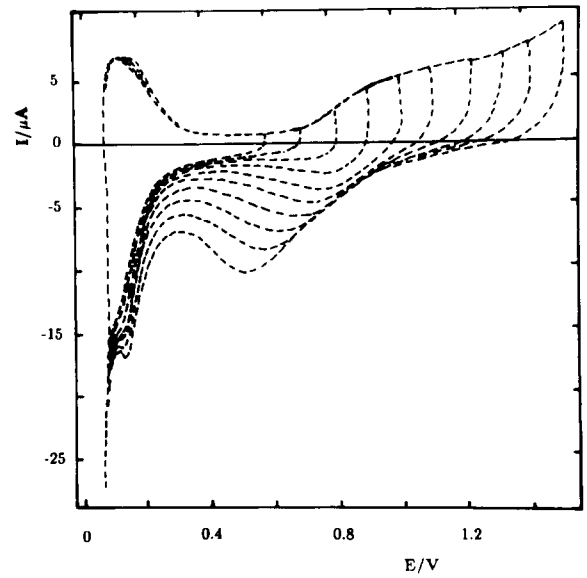

Fig. 10. Potentiodynamic $E-I$ profiles of polycrystalline Rh in $HClO_4 \cdot 5.5H_2O$ at $v = 0.1$ V s^{-1} and $T = 228$ K between $E_c = 0.07$ V and E_a changed stepwise from 1.40 to 0.65 V. Apparent electrode area, 0.53 cm^2.

I for $H_2SO_4 \cdot 12H_2O$ and involves no current peaks such as those shown in Fig. 1. The positive current peak located at about 0.1 V presumably results from H_2 electro-oxidation. In contrast to $H_2SO_4 \cdot 12H_2O$, the O-atom-containing layer in $HClO_4 \cdot 5.5H_2O$ begins at about 0.65 V with a smooth current increase (Fig. 9). The stepwise shift of E_a from 0.6 to 1.5 V indicates that the initial stage for the O-containing layer electroformation on Rh in $HClO_4 \cdot 5.5H_2O$ behaves reversibly, as for $H_2SO_4 \cdot 12H_2O$ at the same T (Fig. 1).

As T is steadly reduced to 228 K, the same voltammetric characteristics are essentially maintained, but the overall voltammetric charge decreases. For frozen $HClO_4 \cdot 5.5H_2O$($T = 228$ K), this charge is smaller by a factor of about eight than that recorded at 298 K. At the lowest T value, a sharp current peak appears at about 0.15 V, preceding the HER, which is caused by the presence of Cl^- anions that result from the instability of the ClO_4^- anion on Rh [12,14–16] and from the proper composition of the electrolyte (Fig. 10).

At $T = 298$ K, the TMV behaviour is comparable with that already described for $H_2SO_4 \cdot 12H_2O$. Either at $T = 298$ K (Fig. 11) or $T = 213$ K (Fig. 12), TMV shows reversible processes in regions I′ and II′. Region I′, which covers the range 0.0–0.4 V, shows the reversible H atom electrosorption reaction; region II′ exhibits the reversible initial stage of the O-containing surface layer and another reversible process at about 1.7 V. This process is enhanced and better resolved in $HClO_4 \cdot 5.5H_2O$ than in $H_2SO_4 \cdot 12H_2O$. The TMV positive charge that results from the reversible process at about 1.7 V is four times greater than those recorded for the reversible H and OH electrosorption

reactions observed at about 0.1 V and 0.8 V respectively. It is worth noting that both reversible processes in region II′ are observed in the frozen electrolyte (Figs. 11 and 12). The capacitive contribution to TMV increases at $T = 213$ K, especially in the range 1.1–1.5 V.

The values of the q_a/q_c charge ratio related to the electrosorption of H atoms, the formation of OH species at about 0.8 V and the reversible system formed at about 1.7 V are always close to unity at all T values. Therefore, in the entire range of T, the difference in potential between the H adatom and oxide regions for $HClO_4 \cdot 5.5H_2O$ is always greater than that for $H_2SO_4 \cdot 12H_2O$. $HClO_4 \cdot 5.5H_2O$ exhibits a smooth rise in the "onset of oxide" region as compared with $H_2SO_4 \cdot 12H_2O$. The current peak at 0.15 V in Fig. 10, which is similar in behaviour to that produced in the desorption of Cl^- ions on Rh [15,16], indicates clearly the presence of Cl^- ions that result from

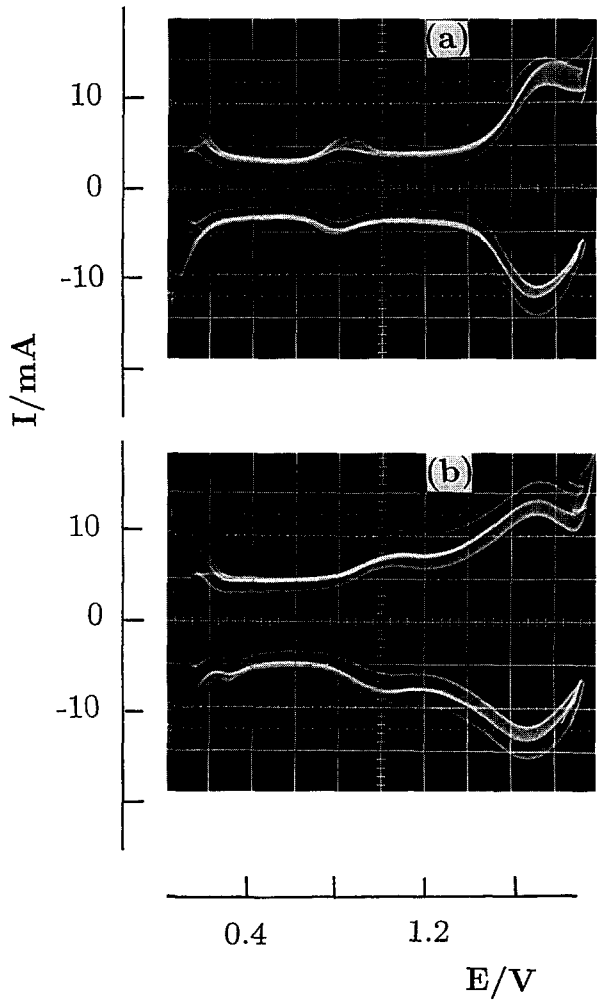

Fig. 11. Triangularly modulated voltammogram recorded between 0.0 and 2.0 V at 0.1 V s^{-1} and $T = 298$ K in $HClO_4 \cdot 5.5H_2O$ with $A = 0.040$ V and $f = 1$ kHz: (a) positive-going potential scan; (b) negative-going potential scan. Apparent electrode area, 0.53 cm^2.

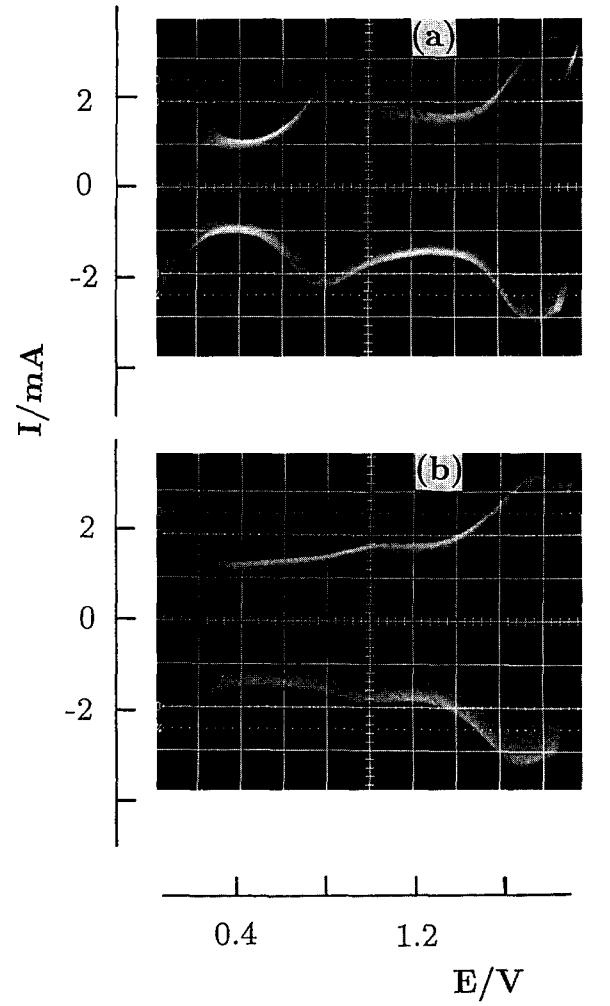

Fig. 12. Triangularly modulated voltammogram recorded between 0.0 and 2.0 V at 0.1 V s^{-1} and $T = 213$ K in $HClO_4 \cdot 5.5H_2O$ with $A = 0.040$ V and $f = 400$ Hz: (a) positive-going potential scan; (b) negative-going potential scan. Apparent electrode area, 0.53 cm^2.

the decomposition of ClO_4^- anions on Rh [12,14,15]. This is consistent with the relatively high initial concentration of Cl^- ions in the electrolyte and the relatively low activation energy of the ClO_4^- anion decomposition reaction on Rh yielding Cl^- ions [14]. The effect of Cl^- ion adsorption on the voltammetric response of Rh in $HClO_4 \cdot 5.5H_2O$ increases as T is reduced.

4. Discussion

4.1. Structure of electrolytes at the electrochemical interface

The temperature effects on H atom and OH electrosorption, O-containing layer formation and electrodissolution, and the redox processes preceding the OER on Rh electrodes depend strongly on the nature of the electrolyte and,

to a lesser extent, on whether the electrolyte is liquid or solid. Therefore, it may be useful to recall certain characteristics of the structures for bulk $H_2SO_4 \cdot 12H_2O$ and $HClO_4 \cdot 5.5H_2O$, and $Rh|H_2SO_4 \cdot 12H_2O$ and $Rh|HClO_4 \cdot 5.5H_2O$ interfaces, in the potential range covered by this work.

The structure of bulk $H_2SO_4 \cdot 12H_2O$ is considered to consist of H-bonded chains [21,22]. This structure would make possible a direct interaction between sulphate anions and the Rh surface, both for the liquid and solid electrolyte. As has been recently demonstrated [13,15], adsorbed sulphate anions on Rh play a key role in the kinetics of electrochemical reactions proceeding in the potential range of our experiments. It was shown further that an adsorbed layer of sulphate anions on Rh(111) is more stable than that on other Rh surfaces, as a result of a more favourable spatial configuration of the anions and the surface water molecule network. The uptake of anions by Rh(111), as concluded from radiochemical data, reaches about 40% of the theoretical maximum coverage for sulphate anion concentrations up to 10^{-3} M. In the absence of Rh surface oxidation, the reversible adsorption of sulphate anions on Rh(111) was verified with respect to the bulk sulphate anion concentration and the electrode potential [13].

However, the crystal structure of bulk $HClO_4 \cdot 5.5H_2O$ has been described as a polyhedral clathrate (pc), where the host lattice is formed by water molecules and the ClO_4^- anion is the guest [23]. The dielectric relaxation of this clathrate is determined by the H_2O framework and the polar characteristics of the guest species, and their ability to interact with the host lattice by H bonding or by the substitution of H_2O molecules. Therefore, for $Rh|HClO_4 \cdot 5.5H_2O$, an anion–Rh surface direct interaction appears to be unlikely for ClO_4^- anions that remain in the host lattice.

However, in this case, the structure of the interface is complicated by the catalytic properties of Rh(100), Rh(111) and Rh (pc) in the processes of ClO_4^- anion reduction in aqueous media yielding Cl^- anions as the main electroreduction product, either at the Rh surface or in the bulk of the solution [14], as concluded from surface analysis, low energy electron diffraction (LEED) and Auger spectroscopy data [14,24]. The rate of ClO_4^- anion electroreduction decreases in the order Rh(100) > Rh(pc) > Rh(111), and the degree of surface coverage ratio for oxygen and chloride in 0.1 M $HClO_4$ at 298 K attains a minimum value at about 0.20 V, i.e. in the potential range related to H atom electrosorption reactions [14]. Furthermore, the apparent heat of activation of perchlorate anion electroreduction on Rh (pc) is 41 kJ mol^{-1}. Therefore, a change in temperature from 298 to 210 K would imply a decrease in the rate of this reaction by a factor of approximately three leading to the unavoidable interference of chloride species with the electrochemical reactions covered in this work, particularly those that occur in the H adatom potential range.

4.2. H electrosorption process on Rh electrodes

The cathodic current contribution recorded at about 0.15 V corresponds to H atom electroadsorption affected by either sulphate anion adsorption or ClO_4^- anion electroreduction, depending on the electrolyte composition.

In $H_2SO_4 \cdot 12H_2O$, as T is decreased, the H atom electroadsorption current peak begins to disappear, the H electrodesorption current peak decreases appreciably and, simultaneously a clear hysteresis in the voltammogram, resulting from anion adsorption, is observed (Fig. 5). This is reflected also in the absence of the reversible pair of current peaks for H atom electrosorption during the negative potential scan.

The strong blockage of Rh adsorption sites by sulphate ions for H electrosorption reactions is consistent with previous results obtained in aqueous HF and H_2SO_4 solutions [9], and can be interpreted through a competition between adsorbable anions and the H atom as expressed by the formal reaction

$$Rh_x(HSO_4^-/SO_4^{2-}) + H_3O^+ + e^- \rightleftharpoons Rh_x(H) + HSO_4^-/SO_4^{2-} + H_2O \quad (1)$$

where x stands for a Rh surface site covered by an adsorbate and the parentheses denote adsorbed species.

The adsorption of sulphate anions on Rh is favoured as compared with other noble metals, probably because of the comparatively lower potential of zero charge [25,26]. The surface coverage of Rh by anions is maximal at the onset of oxide formation [13]. Hence, the greatest inhibition of adsorbed H occurs when E_a is set just at the onset of oxide formation (Fig. 6(b)). The reason that more H adsorbs as E_a becomes more positive (Fig. 6(a)) is that fewer anions are adsorbed as the previous potential scan reaches more positive potentials. As T is reduced, the reversible adsorption of sulphate anions increasingly dominates the kinetics of the H atom electrosorption on Rh.

In $HClO_4 \cdot 5.5H_2O$ the electrochemical behavior of Rh in the H adatom potential region fits into a kinetic scheme in which anions also play a key role. In this case, the H adatom potential range decreases gradually as T is diminished, showing no major changes in the characteristics of the voltammogram, especially when E_a is set at about 0.6 V. The TMV characteristics of the H atom electrosorption remain practically unaltered when T approaches 213 K. In this case, the decrease in the voltammetric charge results from the competing ClO_4^- anion decomposition on Rh, leading to either adsorbed Cl^- or Cl^- anion in solution [14]. Hence, the overall H-atom electrosorption can be simply written as

$$Rh_y(H_2O) + (H_3O)^+ + e^- \rightleftharpoons Rh_y(H) + 2H_2O \quad (2)$$

where y denotes the fraction of Rh surface available for interacting directly with water. Seemingly, at a constant E value, the value of y tends to decrease as T is reduced, causing progressive hinderance of reaction (2).

For both electrolytes, it is reasonable to say that the proton transfer involved in reactions (1) and (2) occurs in an almost completely H-bonded lattice, as if the reorganization energy contribution to the electrochemical process became of little importance as T is decreased.

4.3. Electroformation of the O-containing layer on Rh

The electroformation of the O-containing layer on Rh involves the initial electrosorption of OH species resulting from the underpotential decomposition of water. For $H_2SO_4 \cdot 12H_2O$, the overall reaction can be written as

$$Rh_x(HSO_4^-/SO_4^{2-}) + H_2O \rightleftharpoons Rh_x(OH) + HSO_4^-/SO_4^{2-} + H^+ + e^- \quad (3a)$$

and, for $HClO_4 \cdot 5.5H_2O$, we have

$$Rh_{x'}(Cl^-) + 2H_2O \rightleftharpoons Rh_{x'}(OH) + Cl^- + H_3O^+ + e^- \quad (3b)$$

Reactions (3a) and (3b) are accompanied by a reaction such as

$$Rh_y(H_2O) + H_2O \rightleftharpoons Rh_y(OH) + H_3O^+ + e^- \quad (3c)$$

where x' and y stand for the fractions of Rh surface covered by adsorbed species and by water respectively. This type of reaction involving a simultaneous electron–proton transfer process is already well-established for a number of metal electrodes in aqueous solutions.

According to TMV, reactions (3a) and (3b) are reversible reactions, independently of the electrolyte, over the entire range of T covered in this work. For the solid electrolytes, the proton motion involved in these reactions, either at the reaction interface or in the bulk, can be described as an H transfer between two favourably oriented vicinal water molecules tunnelling the corresponding potential energy barrier. This process, which occurs in ice, can be written as

$$[H_3O^+]_a + [H_2O]_b \rightarrow [H_2O]_a + [H_3O^+]_b \quad (4)$$

where a and b denote two neighbouring water molecules.

The increasing irreversibility of the subsequent stages of the O-containing layer electroformation, which takes place at potentials above 0.9 V, is mainly related to the interference of anion adsorption on the appearance of more stable surface species such as Rh(O). These reactions are also affected by the presence of adsorbed anions on Rh [15,16]. The formation of Rh(O) can be expressed by a formal reaction such as

$$Rh(OH) \rightarrow Rh(O) + H^+ + e^- \quad (5)$$

This represents the oxide layer growth that leads to a presumably hydrated Rh_2O_3 layer, according to

$$2Rh(O) + (z+1)H_2O \rightarrow Rh_2O_3 \cdot zH_2O + 2H^+ + 2e^- \quad (6)$$

The formation of the entire O-containing layer on Rh, according to reaction (6), moves positively as T is decreased. Therefore, anion adsorption hysteresis also occurs in the OH adsorption and desorption potential ranges.

However, the voltammetric electroreduction of the oxide layer in $H_2SO_4 \cdot 12H_2O$ also moves positively when E_a is decreased (Fig. 6). From the two ill-defined voltammetric peaks observed during the negative-going potential scan in TMV (Fig. 7(b)), it can be concluded that the electroreduction of the Rh oxide layer grown up to 1.4 V consists of at least two different species, i.e. Rh oxide and Rh(OH), which are electroreduced at about 0.5 V and 0.8 V respectively.

4.4. Reversible process at about 1.7 V

The second reversible redox process which can be observed in the range 1.6–2.0 V for both electrolytes is somewhat similar to that previously reported for Rh in alkaline solutions [27,28] and 12 M H_2SO_4 [8], when the electrode is potential-cycled and the accumulated charge can be increased by applying a fast potentiodynamic routine [8,27].

It is worth noting that, for both electrolytes, the reversibility of this system appears to be independent of T, at least within the T range covered by this work, and the charge involved in all cases is only a fraction of the charge density expected for the O atom monolayer. Furthermore, the effect of the electrolyte nature and the greater reversibility of the system in solid $HClO_4 \cdot 5.5H_2O$ suggest that, in this case, the kinetics of the reversible process are probably governed by proton mobility, which is actually determined by the electrolyte structure and the presence of Cl^- ions at the reaction interface. Thus, $HClO_4 \cdot 5.5H_2O$ clathrate creates an excess of one proton in the system, in contrast to $H_2SO_4 \cdot 12H_2O$, for which the interaction of H_2SO_4 and H_2O molecules through H bonding leaves the number of protons unchanged. The excess of one proton in $HClO_4 \cdot 5.5H_2O$ could explain why the process at about 1.7 V becomes more reversible in $HClO_4 \cdot 5.5H_2O$ than in $H_2SO_4 \cdot 12H_2O$ (Fig. 12). The mobility of protons in $H_2SO_4 \cdot 12H_2O$ and $HClO_4 \cdot 5.5H_2O$ at low T values can be considered through a tunnelling process which is independent of T rather than through a classical hopping mechanism.

From the above discussion and the fact that the second reversible process always appears at potentials above 1.6 V, irrespective of the substrate metal, it is reasonable to say that the reactant and products involved in the overall electrochemical reaction should be related to H_2O. Then, the second reversible process observed at about 1.7 V is probably related to the equilibrium

$$HO_2 + 3H^+ + 3e^- \rightleftharpoons 2H_2O \quad (7)$$

The standard potential of reaction (7) is $E^0 = 1.65$ V at 298 K [29].

5. Conclusions

(1) The voltammetric behaviour of H and O atom reactions on Rh in $H_2SO_4 \cdot 12H_2O$, in the range 298–198 K, and in $HClO_4 \cdot 5.5H_2O$, in the range 298–210 K, is strongly affected by sulphate anion adsorption for $H_2SO_4 \cdot 12H_2O$ and by electroreduction of perchlorate to chloride anions for $HClO_4 \cdot 5.5H_2O$, as has been reported in the literature at 298 K using more dilute solutions [12–16].

(2) As the temperature is decreased, the effect of anion adsorption becomes more marked, particularly for the H atom electrosorption reactions and the initiation of O-containing layer electroformation. The H atom electroadsorption reaction is practically no longer observed at the lowest T value used in this work, at least in the range 0–0.3 V.

(3) For $H_2SO_4 \cdot 12H_2O$, the voltammetric charge for the initial stages of O-containing layer formation diminishes as T is decreased, as a result of anion adsorption. The same occurs for $HClO_4 \cdot 5.5H_2O$, although the reversibility of the reaction in this case, is maintained over the entire range of T.

(4) For both electrolytes, a reversible process at about 1.7 V is observed over the entire range of T. This process is also affected—although to a minor extent—by the composition of the electrolyte, principally by the adsorption of anions.

(5) The difference in the voltammetric responses of H, OH^- and O atom electrosorption reactions on Rh and Pt already found in aqueous $HClO_4$ and H_2SO_4 solutions at 298 K [9,10] persists in both $H_2SO_4 \cdot 12H_2O$ and $HClO_4 \cdot 5.5H_2O$ over the entire T range.

Acknowledgments

This work was financially supported by the Consejo Nacional de Investigaciones Científicas y Técnicas (CONICET) of Argentina and the Comisión de Investigaciones Científicas de la Provincia de Buenos Aires (CIC). A.E.B. is a Member of the Research Career of CIC.

References

[1] B.E. Conway, in B.E. Conway, R.E. White and J.O'M. Bockris (eds.), Modern Aspects of Electrochemistry, Vol. 16, Plenum, New York, 1985, Ch. 2, p. 103.
[2] U. Stimming, in P.M. Soriaga (ed.), Electrochemical Surface Science, ACS Symposium Series, American Chemical Society, Washington, DC, 1988.
[3] Z. Borkowska, M. Cappadonia and U. Stimming, Electrochim. Acta, 37 (1992) 565.
[4] M.I. Florit, M.E. Martins and A.J. Arvia, J. Electroanal. Chem., 269 (1989) 209.
[5] M.I. Florit and A.J. Arvia, J. Electroanal. Chem., 339 (1992) 281.
[6] W. Bold and M. Breiter, Electrochim. Acta, 5 (1961) 169.
[7] R.V. Marvet and O.A. Petrii, Elektrokhimiya, 3 (1967) 1445.
[8] C. Pallota, N.R. de Tacconi and A.J. Arvia, Electrochim. Acta, 26 (1981) 261.
[9] C. Pallota, N.R. de Tacconi and A.J. Arvia, J. Electroanal. Chem., 159 (1983) 201.
[10] B. Parajon Costa, M.C. Giordano, C. Pallota and A.J. Arvia, J. Electroanal. Chem., 199 (1986) 381.
[11] A. Rakotondrainibe, B. Beden and C. Lamy, J. Electroanal. Chem., 379 (1994) 455.
[12] C.K. Rhee, M. Wasberg, G. Horanyi and A. Wieckowski, J. Electroanal. Chem., 291 (1990) 281.
[13] P. Zelenay, G. Horanyi, C.K. Rhee and A. Wieckowski, J. Electroanal. Chem., 300 (1991) 499.
[14] C.K. Rhee, M. Wasberg, P. Zelenay and A. Wieckowski, Catal. Lett., 10 (1991) 149.
[15] A. Ahmadi, R. Wyn Jones and G. Attard, J. Electroanal. Chem., 350 (1993) 279.
[16] A. Ahmadi, E. Bracey, R Wyn Jones and G. Attard, J. Electroanal. Chem., 350 (1993) 297.
[17] B.E. Conway, H. Angerstein-Kozlowska, F.C. Ho, J. Klinger. B. MacDougall and S. Gottesfeld, Disc. Faraday Soc., 56 (1973) 210.
[18] N.R. de Tacconi, J.O. Zerbino and A.J. Arvia, J. Electroanal. Chem., 79 (1977) 287.
[19] J.O. Zerbino, N.R. de Tacconi and A.J. Arvia, J. Electrochem. Soc., 125 (1978) 1266.
[20] A.E. Bolzán and A.J. Arvia, J. Electroanal. Chem., 341 (1992) 93.
[21] A.F. Wells, Structural Inorganic Chemistry, Part II, Clarendon Press, Oxford, 1986, Ch. 8.
[22] D. Mootz and A. Merschenz-Quack, Z. Naturforsch. B, 42 (1987) 1231.
[23] D. Mootz, E.J. Oellers and M. Wiebcke, J. Am. Chem. Soc., 109 (1987) 1200.
[24] M. Wasberg, M. Hourani and A. Wieckowski, J. Electroanal. Chem., 278 (1990) 425.
[25] N.A. Balashova, A.M. Kossaya and N.T. Gorokhova, Elektrokhimiya, 3 (1967) 656.
[26] A.N. Frumkin and O.A. Petrii, Electrochim. Acta, 20 (1975) 347.
[27] L.D. Burke and E.J.M. O'Sullivan, J. Electroanal. Chem., 93 (1978) 11.
[28] Z. Cataldi, R.O. Lezna, M.C. Giordano and A.J. Arvia, J. Electroanal. Chem., 261 (1988) 61.
[29] A.J. Bard, R. Parsons and J. Jordan (eds.), Standard Potentials in Aqueous Solutions, Dekker, New York, 1985.